AMERICAN SOCIETY FOR MICROBIOLOGY | Journal of Virology®

GENOME REPLICATION AND REGULATION OF VIRAL GENE EXPRESSION

Epstein-Barr Virus miR-BHRF1-3 Targets the BZLF1 3′UTR and Regulates the Lytic Cycle

Devin N. Fachko,[a] Yan Chen,[a] Rebecca L. Skalsky[a]

[a]Vaccine and Gene Therapy Institute, Oregon Health and Science University, Beaverton, Oregon, USA

ABSTRACT Suppression of lytic viral gene expression is a key aspect of the Epstein-Barr virus (EBV) life cycle to facilitate the establishment of latent infection. Molecular mechanisms regulating transitions between EBV lytic replication and latency are not fully understood. Here, we investigated the impact of viral microRNAs on the EBV lytic cycle. Through functional assays, we found that miR-BHRF1-3 attenuates EBV lytic gene expression following reactivation. To understand the miRNA targets contributing to this activity, we performed Ago PAR-CLIP analysis on EBV-positive, reactivated Burkitt's lymphoma cells and identified multiple miR-BHRF1-3 interactions with viral transcripts. Using luciferase reporter assays, we confirmed a miRNA interaction site within the 3′UTR of BZLF1 which encodes the essential immediate early (IE) transactivator Zta. Comparison of >850 published EBV genomes identified sequence polymorphisms within the miR-BHRF1-3 locus that deleteriously affect miRNA expression and function. Molecular interactions between the homologous viral miRNA, miR-rL1-17, and IE transcripts encoded by rhesus lymphocryptovirus were further identified. Our data demonstrate that regulation of IE gene expression by a BHRF1 miRNA is conserved among lymphocryptoviruses, and further reveal virally-encoded genetic elements that orchestrate viral antigen expression during the lytic cycle.

IMPORTANCE Epstein-Barr virus infection is predominantly latent in healthy individuals, while periodic cycles of reactivation are thought to facilitate persistent lifelong infection. Lytic infection has been linked to development of certain EBV-associated diseases. Here, we demonstrate that EBV miR-BHRF1-3 can suppress lytic replication by directly inhibiting Zta expression. Moreover, we identify nucleotide variants that impact the function of miR-BHRF1-3, which may contribute to specific EBV pathologies.

KEYWORDS Epstein-Barr virus, human herpesviruses, lytic cycle, microRNA

Epstein-Barr virus (EBV) is a ubiquitous gamma-herpesvirus that causes infectious mononucleosis and is implicated in several B cell and epithelial cancers as well as lymphoproliferative diseases that occur in immunocompromised patients (1). Generally benign in healthy persons, the virus infects >90% of adults worldwide, undergoing primary lytic infection in epithelial cells of the oropharynx and subsequently establishing latent infection predominantly in B cells (2). Lifelong, persistent infection is coordinated through multiple interactions between cellular and viral factors which facilitate latency and govern intermittent lytic reactivation events critical for maintaining viral reservoirs and enabling virus transmission to new hosts.

The EBV lytic cycle is characterized by sequential expression of immediate early (IE), early, and late genes encoding proteins required for viral replication, the structural proteins necessary for production of new infectious virions, and proteins involved in productive viral egress (reviewed in references 3 and 4). In latent B cells, lytic reactivation can be triggered by antigen-stimulation or plasma cell differentiation (3). Activation of the EBV lytic cascade initiates with expression of two IE viral transcription factors, Zta (encoded by BZLF1) and Rta (encoded by BRLF1), which subsequently transactivate methylated

Editor Lori Frappier, University of Toronto

Address correspondence to Rebecca L. Skalsky, skalsky@ohsu.edu.

The authors declare no conflict of interest.

Received 30 August 2021
Accepted 3 December 2021
Accepted manuscript posted online 8 December 2021
Published 23 February 2022

promoters of early viral genes required for the replication of EBV genomic DNA (4, 5). Zta expression is sufficient to initiate the EBV lytic cycle in most cells, thus the BZLF1 promoter (Zp) is tightly regulated by several cellular transcription factors (6, 7). Additionally, Zta autoregulates itself directly through Z-response elements within Zp (6–8).

Several studies point to a role for lytic infection in the development of EBV-associated cancers (9, 10). In experimental humanized mouse models, viruses lacking BZLF1 that are defective in lytic replication induce fewer lymphomas (11). While increased Zta expression does not necessarily increase tumorgenicity in mouse models (12, 13), defects in EBV genes that erroneously abort the lytic infection cycle and/or enhance early-stage lytic gene expression presumably increase EBV pathogenesis (9, 14, 15). In patients, high EBV loads and elevated antibody titers are associated with increased risk for nasopharyngeal carcinoma (NPC), Hodgkin lymphoma (HL), and potentially certain subtypes of non-Hodgkin lymphoma (NHL) (16, 17). It has been postulated that enhanced lytic infection could increase the pool of infected cells within an individual, thereby increasing the likelihood for developing EBV malignancies (18). An in-depth understanding of how EBV lytic infection is regulated, particularly on a molecular level, is thus an important area of research in targeting EBV-associated diseases.

MicroRNAs are ~22 nucleotide small noncoding regulatory RNAs with essential roles in a multitude of cellular processes. Functioning predominantly through post-transcriptional silencing of their target RNAs, miRNAs are major fine-tuners of gene expression and in humans, target the 3′UTRs of at least 50% of all protein-coding genes (19, 20). Like all human herpesviruses, EBV encodes viral miRNAs which contribute to various aspects of the EBV life cycle and play major roles in modulating antiviral responses (15, 21–23). Of the >40 mature miRNAs expressed by EBV, the majority are produced from clusters within the BART region while three are encoded within the BHRF1 locus (miR-BHRF1-1, miR-BHRF1-2, and miR-BHRF1-3). The BHRF1 miRNAs, in particular, are highly expressed following *de novo* infection of primary B cells and also following lytic reactivation (24, 25), indicating potential functions in transitioning between lytic and latent states.

Multiple studies on human herpesvirus miRNAs have demonstrated that lytic transcripts can be directly regulated by viral miRNAs, suggesting a key role in modulating latency and reactivation processes. EBV miR-BART2, for example, is encoded anti-sense to the viral DNA polymerase BALF5 and targets the BALF5 3′UTR thereby impacting lytic replication (26), whereas EBV miR-BART20-5p was reported to directly silence BZLF1 and BRLF1 expression (27). EBV miRNAs further regulate entry into the lytic cycle through their effects on host genes. In previous *in vitro* work, we have shown that a subset of EBV miRNAs attenuates signaling through the B cell receptor (BCR) by targeting BCR components and consequently, impacts the induction of lytic genes (24). In a similar fashion, miR-BART6 and miR-BART18 target cellular Dicer and MAPK2, respectively, subsequently impacting expression of BZLF1 and BRLF1 in response to lytic reactivation stimuli (28, 29).

Here, we investigated how individual EBV miRNAs impact Zta-mediated induction of the EBV lytic phase. Our study reveals that one of the BHRF1 miRNAs, miR-BHRF1-3, attenuates EBV reactivation by directly targeting the BZLF1 3′UTR. In addition, through analysis of published EBV genomes, we identified sequence variants that impact miR-BHR1-3 function.

RESULTS

EBV miR-BHRF1-3 and miR-BART2 suppress the lytic cycle. To determine whether specific EBV miRNAs impact the ability of the virus to reactivate, we performed a functional screen in 293-2089 cells that are persistently infected with bacmid-derived EBV B95-8 (30). Cells were co-transfected with a plasmid expressing Zta (pSG5-Zta) to directly activate the lytic replication cycle and 21 different EBV miRNAs for which we had available expression vectors (31). Cell-associated viral DNA levels were assayed after 48 h. Of the 21 EBV miRNAs screened, we observed significantly reduced EBV

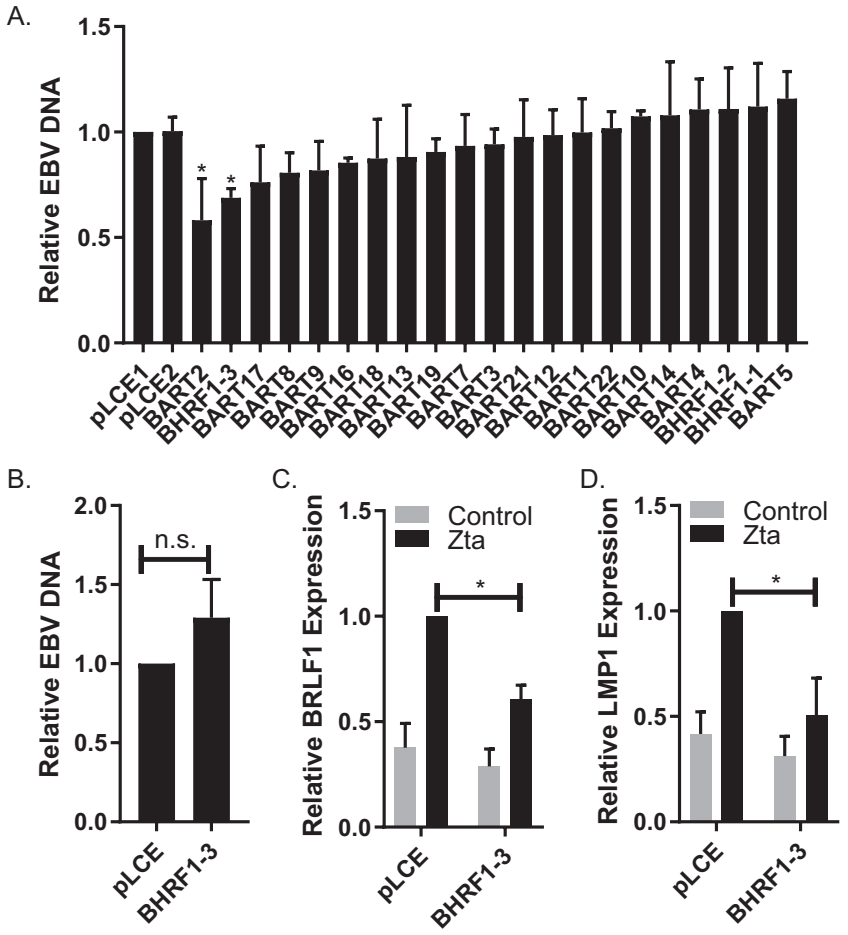

FIG 1 EBV miRNAs impact Z-mediated EBV lytic reactivation. (A) pLCE-based EBV miRNA expression vectors or empty vector control pLCE were co-transfected with a Zta expression vector pSG5-Zta into 293–2089 cells. 48 h posttransfection, genomic DNA was harvested using DNAzol reagent and EBV loads were assayed using qPCR to probe for LMP1. Values are normalized to GAPDH and reported relative to pLCE transfected cells. By Student's *t* test, $^*P < 0.05$, $n = 3$. (B) pLCE-miR-BHRF1-3 or empty vector pLCE was transfected into 293–2089 cells (no Zta expression vector). EBV viral loads were determined as described in Fig. 1A By Student's *t* test, $n = 3$. (C, D) miR-BHRF1-3 attenuates Zta-induction of BRLF1 and LMP1 expression. Control (pcDNA3) or Zta (pSG5-Zta) expression vectors were co-transfected with pLCE-miR-BHRF1-3 into 293–2089 cells. Total RNA was harvested 48 h posttransfection and viral transcripts were assayed by qRT-PCR. Values are normalized to GAPDH and reported relative to Zta transfected empty vector (pLCE) cells. By Student's *t* test, $^*P < 0.05$, $n = 3$.

genome copies (>30%) in the presence of ectopic miR-BART2 and miR-BHRF1-3 relative to control cells transfected with empty vector (pLCE) (Fig. 1A). No significant increases in EBV replication were observed for any of the miRNAs. Decreases in viral DNA loads in the presence of miR-BART2 were anticipated given that miR-BART2-5p targets the EBV BALF5 3'UTR, encoding the viral DNA polymerase processivity factor (26). We therefore focused our attention on miR-BHRF1-3 which has not been closely examined for activity in the EBV lytic cycle.

Ectopic expression of miR-BHRF1-3 in 293–2089 cells in the absence of pSG5-Zta had no impact on steady state viral loads (Fig. 1B), suggesting this miRNA impacts either host and/or viral targets activated during the lytic phase of the EBV life cycle. To examine this further, we measured IE (BRLF1) and late (LMP1) viral gene expression in control and Zta expressing cells (Fig. 1C and D). Notably, Zta induction of BRLF1 was significantly inhibited by ectopic miR-BHRF1-3, suggesting that miR-BHRF1-3 dampens the lytic phase very early on.

We next tested 293-D3 cells that are persistently infected with a miR-BHRF1-3 knockout virus (32). Cells were stably transduced with empty vector (pLCE) or miR-BHRF1-3.

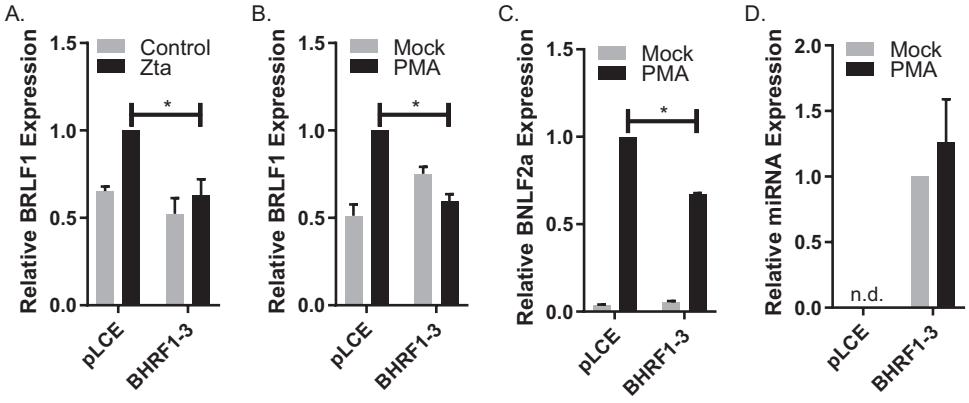

FIG 2 miR-BHRF1-3 attenuates lytic gene expression. (A–C) IE gene BRLF1 and early gene BNLF2a were analyzed by qRT-PCR in 293-EBV-miR-BHRF1-3 KO cells transduced with empty vector (pLCE) or miR-BHRF1-3 expression vector. Lytic cycle was induced by Zta expression (pSG5-Zta) (A) or phorbol12-myristate13-acetate (PMA, 50 ng/ml) (B, C). Values are normalized to GAPDH and reported relative to lytic-induced pLCE transfected cells. By Student's *t* test, $^*P < 0.05$, $n = 3$. (D) miR-BHRF1-3 expression was confirmed by miRNA TaqMan assay. Values are normalized to miR-16 control and reported relative to mock treated miR-BHRF1-3 transduced cells. Shown is the average of three independent experiments. n.d. = not detected.

Following transfection of Zta into these cells, we observed similar patterns as in Fig. 1C; the presence of miR-BHRF1-3 suppressed BRLF1 induction (Fig. 2A). To determine whether miR-BHRF1-3 could suppress the lytic cycle outside the context of Zta, we treated cells with PMA to chemically induce reactivation. Significantly reduced levels of IE (BRLF1) and early (BNLF2a) genes were observed in PMA-treated 293-D3 cells expressing miR-BHRF1-3 (Fig. 2B to D), demonstrating this miRNA attenuates the lytic phase.

Ago PAR-CLIP analysis identifies a miR-BHRF1-3 binding site within the BRLF1/BZLF1 3′UTR. Previous Argonaute (Ago) PAR-CLIP and RISC-IP experiments have identified a few cellular targets for miR-BHRF1-3 in latently infected B cell lines (31, 33, 34), including phosphatase and tensin homolog (PTEN) (35) and TAP2 (34), neither of which play obvious roles in lytic EBV replication. Viral miRNAs expressed by multiple different human herpesviruses (alpha, beta, and gamma) have been shown to repress IE and early genes essential for the lytic cascade (26, 27, 36–39), leading us to hypothesize that miR-BHRF1-3 might act in a similar fashion. In further support of this hypothesis, one early study on herpesvirus miRNAs bioinformatically predicted a binding site for miR-BHRF1-3 in the BZLF1 3′UTR (38).

To experimentally investigate endogenous miR-BHRF1-3 targets during the EBV lytic cycle, we therefore performed Ago PAR-CLIP analysis of naturally infected, EBV-positive Burkitt's lymphoma (BL) cells. Latency I MutuI cells were cultured for 2 h in 4-thiouridine prior to treatment with antibodies against surface IgM to induce reactivation. After 22 h, Ago-bound RNAs were cross-linked at UV 365 nm, immunopurified with antibodies to pan-Ago, ligated to adapters, and sequenced on the Illumina platform (Fig. 3A). Sequencing reads were mapped to the human and EBV genomes and subsequently analyzed with PARalyzer (40) to define Ago interaction sites. Of the annotated Ago interactions, we found that 21% were from cellular protein-coding transcripts (3′UTR/5′UTR/Coding) while a considerable portion of Ago sites (32%) originated from EBV transcripts (Fig. 3B). To focus on miR-BHRF1-3 targets, EBV CLIP'ed regions were scanned for both canonical and non-canonical seed matches (6mer2-7, 6mer3-8, 7mer1A, 7mer2-8, 8mer1A, etc.) to the miRNA. A total of 52 regions were identified (Fig. 3C), 11 of which harbored canonical miR-BHRF1-3 binding sites (≥7mer1A). These 11 sites included a region 58 nt downstream of the BcRF1/BTRF1 polyA signal (sequencing coverage = 87 reads), a region 129 nt downstream of the BDLF4 polyA signal (128 reads), and sites within the BRLF1 (14 reads) and BALF4 (82 reads) coding sequences. Closer inspection of the EBV CLIP'ed regions further revealed a strong binding site for miR-BHRF1-3 in the BRLF1/BZLF1 3′UTR (sequencing coverage = 54 reads) directly adjacent to the stop codon (Fig. 3C).

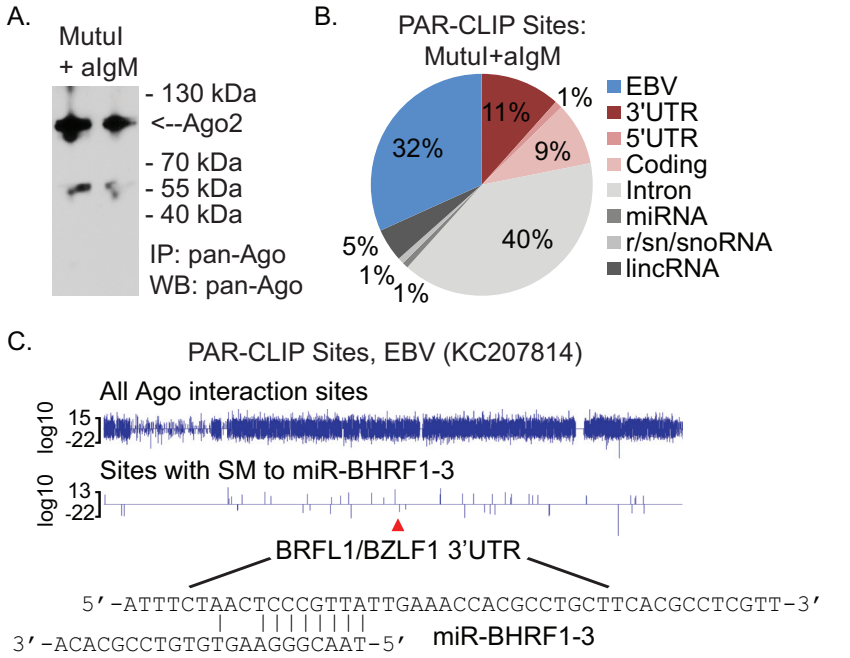

FIG 3 PAR-CLIP analysis of lytic MutuI cells. (A) Immunoblot analysis of Ago in PAR-CLIP lysate. MutuI cells were pretreated with 100 uM 4SU for 2 h prior to reactivation with 2.5 μg/ml anti-IgM for 20 h. Following UV 365 nm cross-linking, Ago-bound 4SU-labeled transcripts were immunopurified (IP) with pan-Ago antibodies. 10% of the PAR-CLIP lysate was analyzed by immunoblot to confirm Ago IP (lanes loaded in duplicate). (B) Distribution of Ago PAR-CLIP sites identified in anti-IgM treated MutuI cells. Reported are Ago interactions that map to EBV and annotated protein, small RNA, or lincRNA coding regions of the human genome (HG19). (C) Ago interactions identified for EBV and sites with seed-matches (SM) to miR-BHRF1-3. Highlighted is the CLIP'ed region of the BRLF1/BZLF1 3'UTR with the miR-BHRF1-3 binding site.

miR-BHRF1-3 targets the BZLF1 3'UTR and impacts virus production. The entire BZLF1 transcript overlaps the BRLF1 3'UTR sequence (Fig. 4A), raising the question of whether miR-BHRF1-3 potentially targets BZLF1 3'UTR, BRLF1 3'UTR, or both. Of note, the Zta expression vector (pSG5-Zta) tested in Fig. 1 and 2 contains the full BZLF1 gene, including the 3'UTR with an intact miR-BHRF1-3 binding site. Moreover, given the location of the BRLF1/BZLF1 CLIP'ed region, spatial preferences for miRNA binding sites (including viral miRNA binding sites), as well as observations that miRNA seed match sites residing close to stop codons frequently mediate strong RNA silencing (20, 33, 41), we hypothesized that miR-BHRF1-3 is likely to regulate BZLF1.

To test this hypothesis, we first generated a luciferase reporter that contains the full BZLF1 3'UTR with the miR-BHRF1-3 seed-match site plus 18 nt upstream to account for any potential miRNA interactions from the 3' end of miR-BHRF1-3. A miRNA seed-match site mutant was generated in parallel (Fig. 4B). Luciferase reporters were subsequently co-transfected with pLCE or the miR-BHRF1-3 expression vector into 293T cells. The presence of miR-BHRF1-3 significantly suppressed luciferase activity from the BZLF1 3'UTR reporter, whereas mutation of the miRNA binding site restored activity (Fig. 4C).

Next, to specifically investigate the impact of miR-BHRF1-3 on Zta protein, we generated two BZLF1 constructs: one in which the BZLF1 3'UTR is deleted (dUTR) and a second expressing the full length BZLF1 gene with an intact 3'UTR (FL). Through Western blot analysis, we observed that co-transfection of miR-BHRF1-3 reduced Zta expression from the FL construct (Fig. 4D and E). Surprisingly, removal of the 3'UTR not only abrogated miRNA suppression, but led to increased protein expression in the presence of miR-BHRF1-3. Although further investigation will be needed, we speculate that some cellular targets of miR-BHRF1-3 potentially negatively regulate Zta protein.

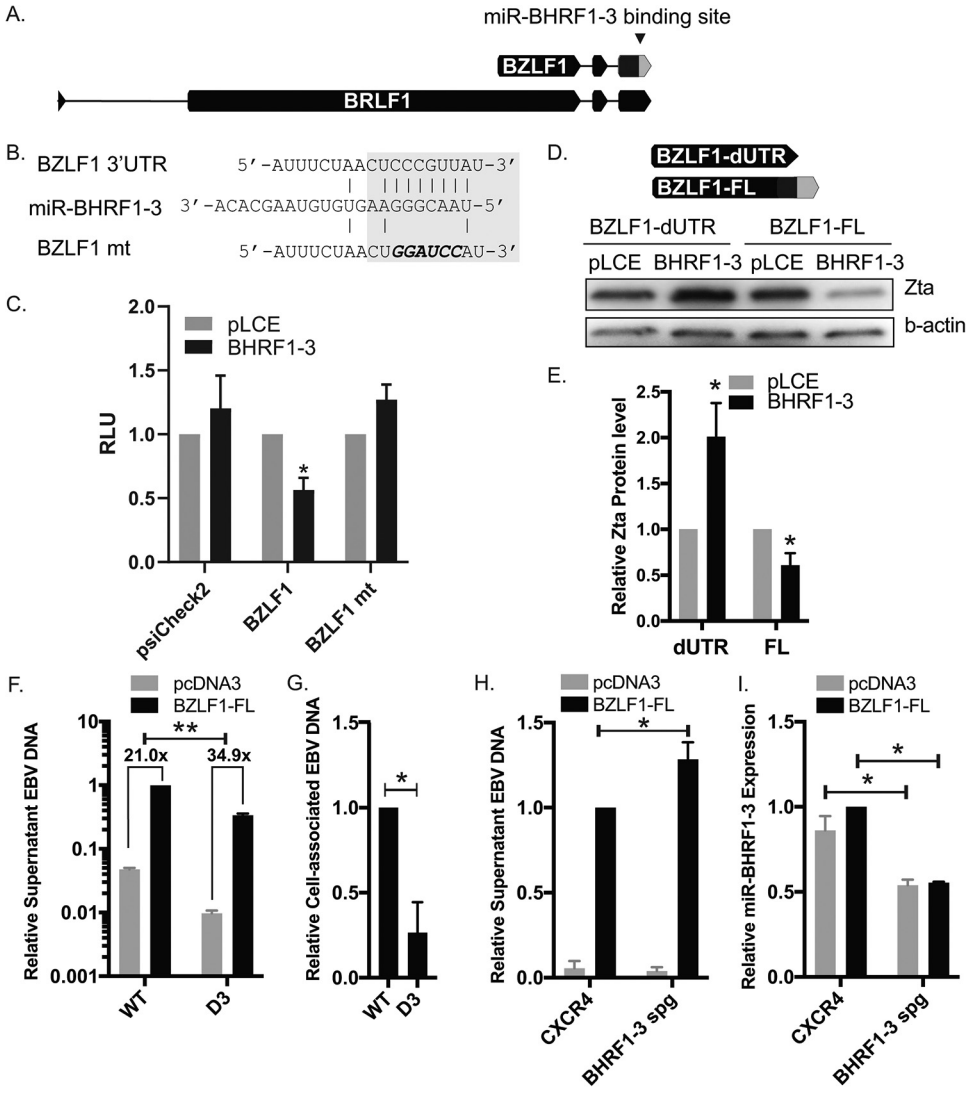

FIG 4 miR-BHRF1-3 targets the BZLF1 3′UTR. (A) Schematic of the BZLF1 and BRLF1 transcripts. The entire BZLF1 transcript overlaps with the BRLF1 3′UTR. (B) Regions of the BZLF1 3′UTR highlighting the miR-BHRF1-3 binding site. The miR-BHRF1-3 seed match site was mutated to a BamHI restriction enzyme site in the BZLF1 mt to disrupt miRNA binding. (C) miR-BHRF1-3 significantly reduces BZLF1 3′UTR activity, while mutation of the miR-BHRF1-3 binding site restores activity. pLCE or the miR-BHRF1-3 expression vector was co-transfected with the wildtype or mutant BZLF1 3′UTR in psicheck2 into 293T cells. 72 h posttransfection, cells were lysed and assayed for dual luciferase activity. Reported is the average of three independent experiments. By Student's *t* test, $^{*}P < 0.05$. RLU = relative light units. (D) Zta protein expression is impacted by the presence of miR-BHRF1-3. 3′UTR-deleted BZLF1 (dUTR) or full-length (FL) BZLF1 gene was co-transfected with pLCE or the miR-BHRF1-3 expression vector into 293T cells. 72 h post-tranfection, cells were lysed and Zta protein was detected by immunoblot. Beta-actin levels are shown as loading controls. E. Band intensities from three independent Zta immunoblots (example shown in D.) were quantified using NIH ImageJ, normalized to loading controls, and reported relative to pLCE-transfected cells. By Student's *t* test, $^{*}P < 0.05$, $n = 3$. F. 293-EBV2089 WT or D3 cells were transfected with pcDNA3 empty vector or pcDNA3-BZLF1-FL to induce EBV lytic replication. Supernatant was collected at 72 h posttransfection and viral DNA loads were determined by qPCR using LMP1 standard curve. Values are reported relative to BZLF1-transfected wildtype cells. Fold changes between each pair of pcDNA3 control and BZLF1-transfected cells are labeled. Asterisks indicate significant increases in supernatant viral DNA from D3 cells transfected with BZLF1-FL compared to WT cells when normalized to pcDNA3 background levels (mean of 34.9-fold vs 21-fold). By Student's *t* test, $^{**}P = 0.005$, $n = 3$. G. Cell-associated viral DNA from 293-EBV2089 WT or D3 cells were determined by qPCR as previously described. By Student's *t* test, $^{*}P < 0.05$, $n = 3$. H. 293-EBV2089 WT cells were co-transfected with pcDNA3 or BZLF1-FL and a sponge inhibitor against miR-BHRF1-3 (BHRF1-3 spg) or pLCE-CXCR4 control sponge. EBV DNA in supernatant were determined as previously described and reported relative to BZLF1-transfected CXCR4 control cells. By Student's *t* test, $^{*}P < 0.05$, $n = 6$. I. miR-BHRF1-3 expression levels in control or sponged 293-EBV2089 WT cells were determined by TaqMan assays, normalized to miR-16 internal control and reported relative to BZLF1-transfected CXCR4 control cells. By Student's *t* test, $^{*}P < 0.05$, $n = 3$.

Together, these results confirm that miR-BHRF1-3 targets the BZLF1 3′UTR directly through a canonical seed-match site and regulates Zta protein levels.

To examine Zta effects on virus production in the presence and absence of miR-BHRF1-3, we next introduced the BZLF1-FL construct into 293-EBV2089 (WT) or 293-D3 (D3) cells and assayed virion levels in the supernatant. Surprisingly, compared to WT cells, less virus was detected in the supernatant of D3 cells (Fig. 4F). Consistent with observations above, however, the magnitude of lytic induction following BZLF1-FL transfection was significantly greater in cells lacking miR-BHRF1-3 (34.9-fold in D3 vs 21-fold in WT, Fig. 4F). Assessment of cell-associated viral loads in untreated cells revealed significantly lower EBV DNA copies in 293-D3 which explains the reduced virus production (Fig. 4G). We therefore focused on WT cells and introduced a miRNA sponge inhibitor to block activity of miR-BHRF1-3. Loss of miR-BHRF1-3 function significantly enhanced virus levels detected in the supernatant following co-transfection of BZLF1-FL (Fig. 4H), demonstrating that miR-BHRF1-3 regulates progeny virus production in the presence of Zta. miRNA knockdown is shown in Fig. 4I.

Sequence polymorphisms in the miR-BHRF1-3 precursor impact miRNA expression and function. Studies on KSHV sequence variations have identified SNPs in the miRNA loci that mechanistically interfere with Drosha and/or Dicer processing of precursor miRNAs and notably, track with clinical phenotypes (42, 43). SNPs have been documented in the EBV BART miRNA loci for NPC isolates from Chinese and Indonesian patients which impact expression of individual BART miRNAs (44, 45). We therefore sought to address whether SNPs occurred in the miR-BHRF1-3 region that potentially impact its expression and/or ability to regulate IE gene expression. EBV-positive Raji cells, for example, were reported to contain a single nucleotide mutation within the miR-BHRF1-3 precursor that severely limits detection of the mature miRNA (46). Other early studies on EBV BHRF1 miRNAs in virus isolates from 12 BL cell lines documented multiple sequence polymorphisms in the miR-BHRF1-3 precursor (25). The observed nucleotide changes in the miR-BHRF1-3 stem-loops did not appear to impact overall miRNA expression levels (25); however, miRNA functional activity was not evaluated.

To more comprehensively examine polymorphisms in the miR-BHRF1-3 precursor, sequences were extracted from 880 documented EBV isolates and published EBV genomes available in the NCBI nucleotide database and aligned using Clustal Omega (47). Our analysis included viral sequences from type 1 and type 2 EBV strains, BL, NPC, EBV-associated gastric cancers, chronic active EBV (CAEBV), and NK T cell lymphomas. Two major miR-BHRF1-3 variants were identified that accounted for >89% of sequences (Fig. 5A). Intriguingly, these two variants differ by a G-to-A nucleotide change occurring in the terminal loop region (Fig. 5B). Moreover, this G-to-A SNP is present in the C666 (KC617875), GD2 (HQ020558), and M81 (KF373730) strains isolated from NPC (48). Three additional minor variants, each present in >1% of sequences, were identified which contain nucleotide substitutions within the mature miRNA sequence (Fig. 5A). Predicted mFold (49) RNA secondary structures, shown in Fig. 5B, indicate that these sequence variants can form stable pre-miRNA hairpins. Through further analysis of 5′ and 3′ flanking regions directly adjacent to the miR-BHRF1-3 precursor, we additionally observed a C-to-A sequence variation that occurs 55 nt downstream of the miR-BHRF1-3 pre-miRNA which is present in 12.4% of EBV genomes, including the EBV B95-8 strain (Fig. 5B and not shown). Additionally, we observed an A-to-T variation that occurs 17 nt upstream of the miR-BHRF1-3 pre-miRNA and is present in the C666 and M81 strains.

To determine whether the observed nucleotide changes could impact functional activity of miR-BHRF1-3, we generated constructs encoding the primary miR-BHRF1-3 regions representative of EBV WT, B95-8, C666/M81, and HKNPC strains. miRNA expression vectors were transfected into 293T cells along with a miRNA reporter containing two tandem perfect binding sites for miR-BHRF1-3 within the firefly luciferase 3′UTR. As expected, expression of WT or B95-8 miR-BHRF1-3 resulted in >90% luciferase inhibition (Fig. 5C). In contrast, the C666/M81 miR-BHRF1-3 resulted in approximately 75% knockdown of the reporter while the HKNPC miR-BHRF1-3 showed no significant knockdown (Fig. 5C). We then tested the miR-BHRF1-3 variants against the BZLF1

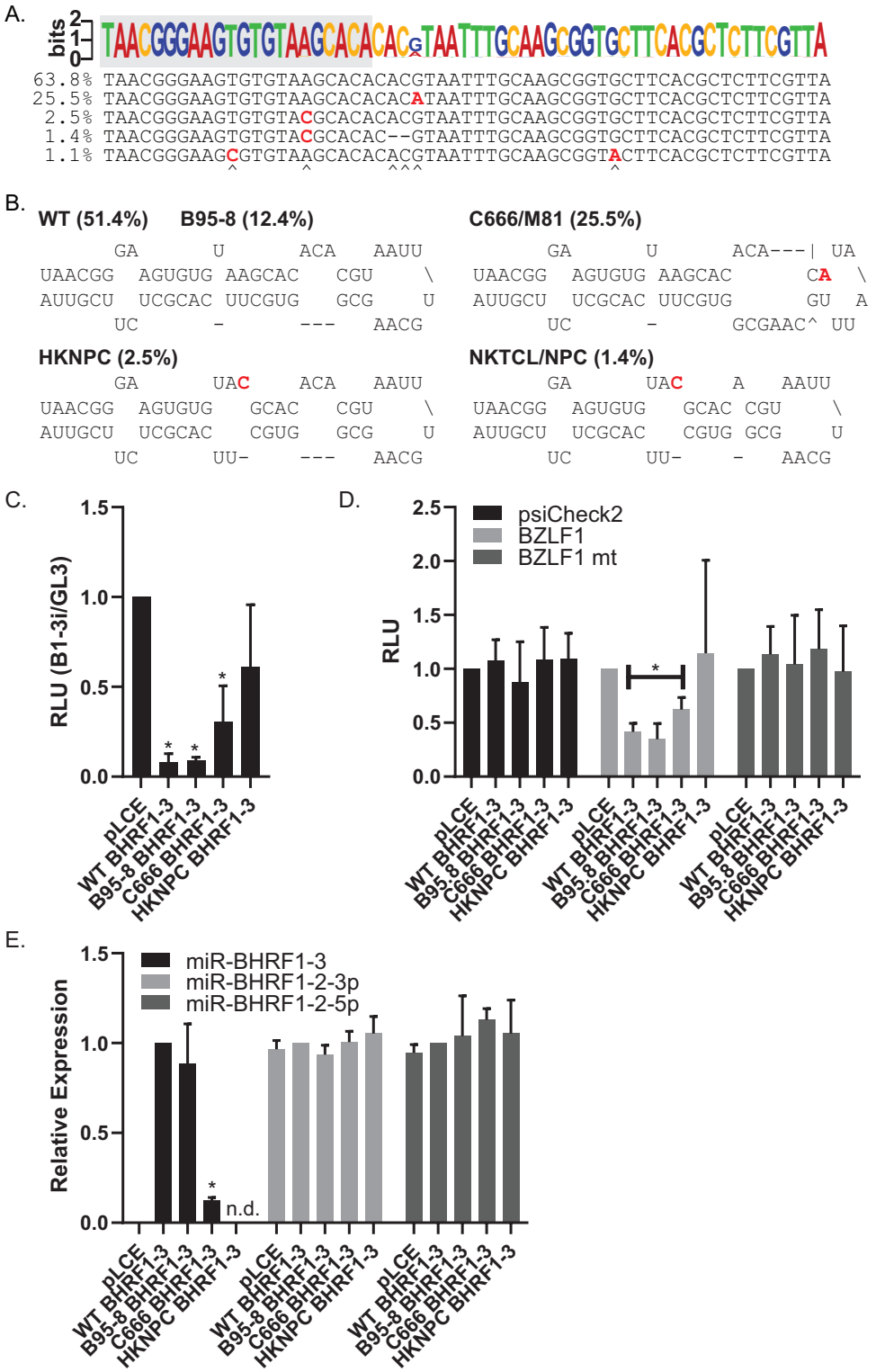

FIG 5 Sequence polymorphisms in the BHRF1-3 miRNA locus impact function and expression. (A) Graphical representation of sequence variations observed in the miR-BHRF1-3 precursor (weblogo.berkley.edu). Of the 880 EBV genomic sequences analyzed, 25.5% contain a G-to-A variation at nucleotide position 27. Sequence alignments of the top five variants illustrate individual nucleotide changes, highlighted in red. (B) Predicted secondary structures for miR-BHRF1-3 precursors representing EBV WT, B95-8, C666, or HKNPC strains. Nucleotide variations are highlighted in red. (C) Nucleotide changes affect miR-BHRF1-3 functional activity. MiRNA expression vectors were transfected into 293T cells with a reporter construct containing two perfect binding sites to miR-BHRF1-3. 72 h posttransfection, cells were lysed and assayed for dual luciferase activity.

(Continued on next page)

3′UTR. Similar to the miRNA reporter, both C666/M81 and HKNPC variants were significantly impaired in their abilities to silence the BZLF1 reporter compared to WT or B95-8 miR-BHRF1-3 (Fig. 5D).

We subsequently investigated whether mature miRNA expression from the miR-BHRF1-3 variants was impacted by the nucleotide differences. Individual vectors were transfected into 293T cells, total RNA isolated at 72 h, and miRNA expression levels were assessed by qRT-PCR. A vector encoding the BHRF1-2 miRNAs (pLCE-miR-BHRF1-2) was used as an internal control. Comparable miR-BHRF1-3 levels were detected for the EBV WT and B95-8 vectors (Fig. 5E). Expression of C666/M81 miR-BHRF1-3, however, was severely reduced while HKNPC miR-BHRF1-3 was not even detectable (Fig. 5E). These results demonstrate that sequence variations in pathogenic EBV strains abolish miR-BHRF1-3 expression and consequently impact miRNA silencing of the BZLF1 3′UTR.

Nucleotide variations in the BZLF1 3′UTR do not significantly alter miRNA-mediated silencing. Natural polymorphisms in the BZLF1 gene, particularly the promoter region, have been identified in EBV strains isolated from nasopharyngeal carcinoma, gastric carcinoma, and AIDS-related lymphoma (18, 48). Notably, the V3 variant, present in type 2 EBV strains, generates an NFAT binding site in the BZLF1 promoter that enhances Zta expression and is linked to increased lytic replication (18). Altered post-transcriptional regulation of IE gene expression, such as disrupted miRNA-mediated inhibition of BZLF1, could potentially result in enhanced lytic replication phenotypes. To further investigate this idea, we examined the 880 EBV sequences for variants within the BZLF1 3′UTR. Two SNPs were identified, illustrated in Fig. 6A Intriguingly, 25% of the EBV genomes contained a C-to-T SNP within the confirmed miR-BHRF1-3 interaction site, directly adjacent to the seed-match region which could potentially enhance miRNA silencing of BZLF1 through increased Watson-Crick base-pairing (Fig. 6B). Representative strains containing this SNP include VGO (KP968260), GD1 (AY961628), and YCCEL1 (AP015016).

To determine how the C-to-T VGO/GD1/YCCEL1 SNP might impact post-transcriptional regulation of the BZLF1 3′UTR, we generated a luciferase reporter and tested activity in the presence of miR-BHRF1-3. While significant knockdown was observed for both 3′UTRs, compared to the level of knockdown achieved with the major BZLF1 3′UTR sequence, we found that the SNP only moderately enhanced silencing by $>$15% in the presence of miR-BHRF1-3 (Fig. 6C). These observations indicate that while multiple nucleotide variants do occur in BZLF1 gene, unlike the V3 variant within the promoter region, the major variants within the BZLF1 3′UTR are unlikely to significantly impact lytic gene expression.

Conserved targeting of the BZLF1 3′UTR by lymphocryptovirus BHRF1 miRNAs (Fig. 7). EBV is a member of the Lymphocryptoviridae family. Among closely related lymphocryptoviruses that infect Old World primates, the sequences of miR-BHRF1-1 and miR-BHRF1-2 pre-miRNAs are highly conserved (31, 50). Intriguingly, EBV miR-BHRF1-3 lacks sequence homology to known and predicted nonhuman primate (NHP) lymphocryptovirus BHRF1 miRNAs, but has positional homologs within these viruses. Figure 7A illustrates the BHRF1 miRNAs in EBV and the related rhesus LCV; rLCV miR-rL1-17 is a positional homolog of miR-BHRF1-3.

To determine whether NHP LCV miR-BHRF1-3 homologs might also target BZLF1, we scanned the BZLF1 3′UTR sequences of lymphocryptoviruses that infect rhesus (NC_006146) and cynomolgous (KP676001) macaques. Intriguingly, canonical seed-match binding sites were identified for both miR-BHRF1-3 homologs (Fig. 7B and C), suggesting

FIG 5 Legend (Continued)
Shown is the average of three independent experiments. (D) C666 miR-BHRF1-3 is functionally impaired in BZLF1 3′UTR inhibition. Values are normalized to renilla and pLCE control, and reported relative to psiCheck2 empty vector. Significance shown is C666 miR-BHRF1-3 compared to WT miR-BHRF1-3. By Student's *t* test, $^*P < 0.05$. RLU = relative light units. E. miRNA expression levels in 293T cells co-transfected with individual miR-BHRF1-3 vectors and a miR-BHRF1-2 expression vector as an internal control. Total RNA was harvested at 72 h posttransfection and miRNAs were assayed by qRT-PCR. Shown is the average of three independent experiments. Values are normalized to cellular miR-16 and reported relative to WT. By Student's *t* test, $^*P < 0.05$. n.d. = Not detected.

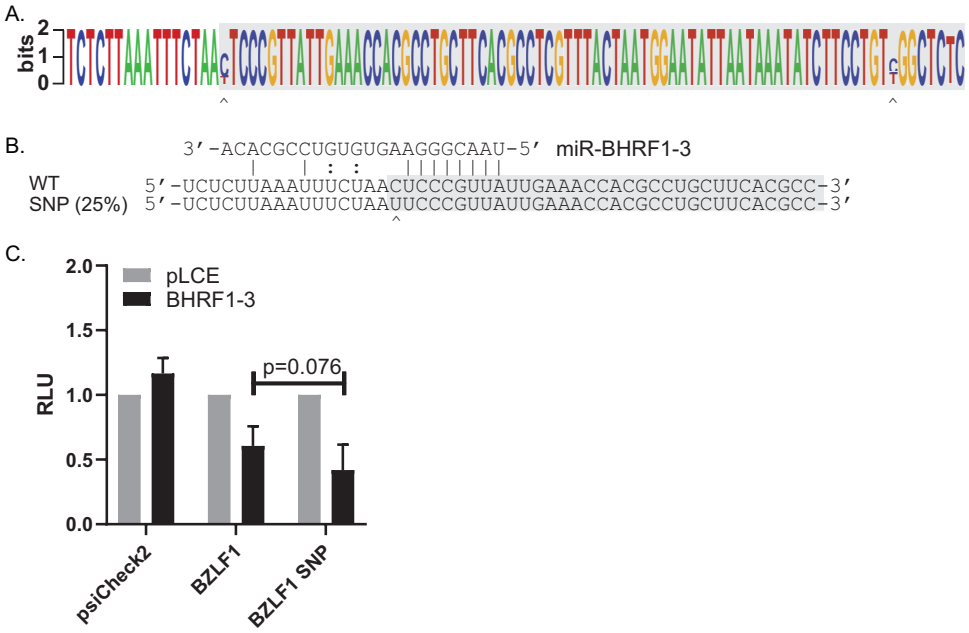

FIG 6 SNP in the BZLF1 3′UTR moderately impacts activity. (A) Sequence logo illustrating the location of two SNPs within the BZLF1 3′UTR based on analysis of 880 EBV sequences. (B) Illustration showing miR-BHRF1-3 binding to BZLF1 3′UTR and where the C-to-T SNP sits in relation to the miR-BHRF1-3 seed-match site. SNP indicated by caret. (C) The BZLF1 SNP moderately enhances knockdown in the presence of miR-BHRF1-3. 293T cells were co-transfected with miR-BHRF1-3 vector and BZLF1 WT or SNP vectors. 72 h posttransfection, cells were lysed and assayed for dual luciferase activity. Shown is the average of three independent experiments. RLU = relative light units.

that regulation of Zta expression is a conserved function for these viral miRNAs. To gain experimental evidence for this hypothesis, we generated a vector encoding rLCV miR-rL1-17 and confirmed expression by qRT-PCR (Fig. 7D). The rLCV BZLF1 3′UTR was subsequently cloned in psiCheck2. Co-expression of miR-rL1-17 with the rLCV BZLF1 reporter resulted in significant knockdown of luciferase activity (Fig. 7E). We included the rLCV homolog of EBV miR-BART20, miR-rL1-16, in our assays since miR-BART20 was previously reported to target EBV BZLF1 3′UTR (27). However, despite the EBV and rLCV miRNAs being >95% conserved at the sequence level, the rLCV BZLF1 reporter was not responsive to ectopic miR-rL1-16 (Fig. 7E). Mutation of the predicted seed-match site for miR-rL1-17 rescued activity (Fig. 7F), demonstrating that regulation of the BZLF1 3′UTR is a conserved function for LCV BHRF1 miRNAs.

DISCUSSION

Lytic replication is an integral part of the EBV life cycle and highly regulated at the molecular level. Here, we investigated how one of the EBV BHRF1 miRNAs, miR-BHRF1-3, suppresses the lytic cycle and discovered a novel link between this miRNA and expression of the Zta IE transactivator. Moreover, we demonstrate that this interaction is a conserved regulatory mechanism encoded within closely related lymphocryptoviruses and thus, likely to play an important role in virus replication *in vivo*.

Direct regulation of IE gene expression by viral miRNAs has been previously described for a number of herpesviruses. Gray et al. and subsequently, confirmed by Murphy et al., first demonstrated this idea for a human cytomegalovirus (hCMV) encoded miRNA, miR-UL112-1, which suppresses expression of the hCMV major IE protein IE72 (also called IE1) (37, 38). IE72 promotes transcriptional activation of early and late genes needed for virus replication. Similar to our findings here with EBV miR-BHRF1-3, ectopic miR-UL112-1 reduced viral genome copies in hCMV infected cells, and intriguingly, this function appears to be conserved in the closely related chimpanzee CMV (37). Alpha-herpesviruses, such as HSV1, also encode miRNAs to dampen IE gene expression. HSV1 miR-H2-3p downregulates

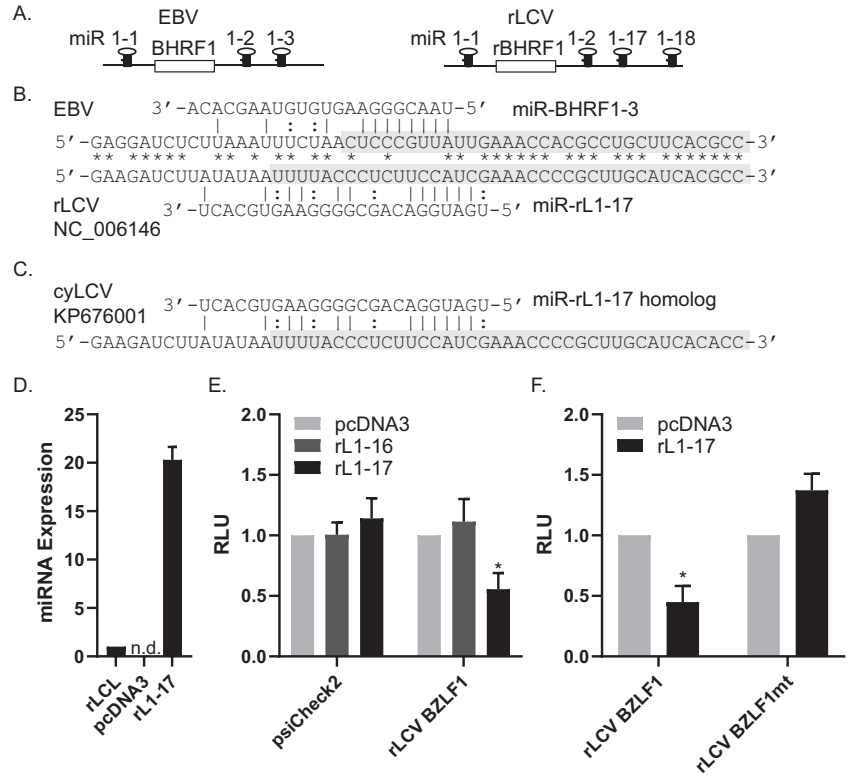

FIG 7 BHRF1 miRNA regulation of the BZLF1 3′UTR is conserved in lymphocryptoviruses. (A) Schematic illustration of the EBV and rLCV BHRF1 loci encoding miRNAs. (B) Alignment of the EBV and rLCV BZLF1 regions with confirmed and predicted miRNA sites for miR-BHRF1-3 and miR-rL1-17, respectively. Asterisks indicate nucleotide conservation. The start of the BZLF1 3′UTR for each virus is highlighted in gray. (C) Schematic showing the predicted binding site for the miR-rL1-17 homolog in the cynomologous LCV BZLF1 3′UTR. D. Validation of rLCV miRNA expression. RNA was isolated from 293T cells transfected with either pcDNA3 or pcDNA3-rL1-17 or from latently infected rLCLs. miRNA expression was assayed by qRT-PCR. Values are normalized to cellular miR-16 and reported relative to miR-rL1-17 levels in rLCLs. Reported is the average of three experiments. n.d. = Not detected. E and F. The rLCV BZLF1 3′UTR is targeted by miR-rL1-17. 293T cells were co-transfected with miRNA expression vectors and rLCV BZLF1 constructs as indicated. 72 h posttransfection cells were lysed and assayed for dual luciferase activity. Shown is the average of three independent experiments. By Student's *t* test, $^*P < 0.05$. RLU = relative light units.

expression of ICP0 whereas miR-H6 targets ICP4 (39). Likewise, for gamma-herpesviruses, the KSHV lytic transactivator Rta which is critical for initiating the lytic cascade is subject to regulation by multiple KSHV miRNAs. *In vitro* luciferase reporter assays have shown that miR-K12-9-5p and miR-K12-7-5p can directly target the KSHV Rta/ORF50 3′UTR (36, 51, 52). Collectively, these studies have put forth the notion that viral miRNA-mediated silencing of IE gene expression is advantageous in fine-tuning temporal control over the lytic cascade for effective progression of herpesvirus replication and further governs the establishment of latency.

An intriguing question that arises from observations here as well as other studies is when is viral miRNA regulation of Zta most critical during EBV infection? One previous study reported that miR-BART20-5p directly targeted BZLF1 and BRLF1 3′UTRs as miRNA mimics reduced activity of luciferase reporters harboring these 3′UTRs (27). Moreover, in EBV-infected gastric cancer cell lines treated with TPA to induce the lytic cycle, a mimic of miR-BART20-5p reduced Zta and Rta proteins levels whereas a miR-BART20-5p inhibitor enhanced levels (27), suggesting that miR-BART20-5p acts to repress IE gene expression in response to reactivation triggers. Mutational inactivation of the three BHRF1 miRNAs or the clustered BART miRNAs impacts the ability of EBV to efficiently immortalize B cells *in vitro*; however, miRNA-knockout viruses still retain the ability to establish a form of latent infection in lymphoblastoid cell lines (LCLs) (23, 30,

53, 54). While spontaneous lytic replication has been observed in LCLs upon deletion of the BART miRNAs- in particular, BART Cluster 1 encoding miR-BART3, 4, 1, 15, 5, 16, 17, and 6 (23, 54), LCLs infected with BHRF1 miRNA knockout viruses lacking individual BHRF1 miRNAs or all three do not appear to spontaneously reactivate (30, 53). Although protein expression was not evaluated, assessment of BZLF1 transcript levels in LCLs by semi-quantitative PCR revealed no significant changes upon deletion of the BHRF1 miRNAs (53). Furthermore, comprehensive Ago CLIP studies examining miRNA targets in NPC, BL, and LCLs latently infected with EBV B95-8 (lacking miR-BART20), BHRF1 miRNA knockout viruses (lacking miR-BHRF1-3), or virus strains expressing all EBV miRNAs (including miR-BHRF1-3 and miR-BART20) did not capture any miRNA interactions with the BZLF1 3′UTR (31, 33, 55, 56). Of note, these CLIP studies also did not capture interactions between miR-BART2-5p and BALF5. Thus, post-transcriptional miRNA-mediated mechanisms seem to play less of a role in regulating Zta during the maintenance of established latent infection, at least *in vitro*. In this context, it is possible that transcriptional repression of the BZLF1 promoter and/or post-translational modifications play a more dominant role in Zta control.

Prior Ago CLIP studies were performed exclusively on latently infected cells which can explain why latent, not lytic, viral transcripts have largely been identified as viral miRNA targets to date (31, 33, 55, 56). Here, we show that miR-BHRF1-3 impacts EBV viral loads when co-expressed with Zta and provide experimental Ago CLIP-based evidence that miR-BHRF1-3 interacts directly with the BZLF1 3′UTR when latent BL cells are reactivated. It is worth noting that, while not investigated in detail, we did identify multiple Ago interaction sites for other EBV lytic transcripts (Fig. 3). These sites remain to be functionally interrogated; however, it is likely that additional key interactions between EBV transcripts and miRNAs with roles in the lytic cycle will be defined in future experiments. Moreover, these observations support the hypothesis that lytic transcripts such as BZLF1 are subject to viral miRNA regulation not during the latent period of infection, but during transitional stages of the virus life cycle.

EBV encodes at least 80 lytic proteins and nine latent proteins which can elicit host antiviral responses and act as targets for cytotoxic T cell responses (CTL) (57). As $CD8^+$ T cell responses against EBV-infected cells are detrimental to persistence, counteractive measures must be encoded within the virus. Recent studies demonstrate that a major function of EBV miRNAs is attenuation of adaptive immune responses which occurs by limiting $CD8^+$ T cell control (23, 34). In the absence of EBV miRNAs, $CD8^+$ T cell recognition of infected B cells is substantially increased (23, 34, 57). Presumably, this phenotype is attributed in part to upregulated cellular targets of EBV miRNAs, such as TAP2 regulated by miR-BHRF1-3 and miR-BART17 which contributes to antigen processing and MHC class I presentation to $CD8^+$ T cells (34). An alternate explanation for these observed phenotypes is that EBV miRNAs regulate expression of viral antigens. Thus, in the absence of the viral miRNAs, viral proteins that are aberrantly expressed, particularly proteins such as Zta that activate multiple viral gene products, could potentially enhance the antigenic load and alter the course of infection.

A notable finding in this study is that SNPs within the EBV miR-BHRF1-3 precursor detrimentally impact both its expression and function. Moreover, these SNPs are present in virus isolates from NPCs, lymphomas, and patients with CAEBV- a rare complication of unresolved chronic EBV infection characterized by prolonged high viral DNA loads (58). Given that the SNPs in miR-BHRF1-3 impact its ability to efficiently target the BZLF1 3′UTR (Fig. 5), it is possible that aberrant post-transcriptional regulation of Zta expression contributes in part to these diseases. In addition to the viral target identified here, miR-BHRF1-3 has several experimentally identified cellular targets (RAS-related protein 2A, MATR3, CXCL11, PTEN, TAP2, etc.) (33–35, 59); however, to date, the roles of these interactions in EBV infection are largely unexplored. Of note, one such target of miR-BHRF1-3, RAS-related protein 2A, was found to be one of the most upregulated genes in high-grade versus low-grade tumors from 124 NPC patients (60). Moreover, miR-BHRF1-3 targets PTEN, a tumor suppressor involved in cell proliferation,

apoptosis, and metabolic reprogramming (33, 35). It is possible that deleterious miR-BHRF1-3 activity accounts for some of the gene expression changes observed in NPCs and other EBV cancers. Future studies will be necessary to understand the exact roles of these SNPs in EBV pathogenesis.

In conclusion, this study provides new insight into the post-transcriptional mechanisms regulating Zta expression and further reveals virally-encoded genetic elements that play a functional role in orchestrating the lytic phase.

MATERIALS AND METHODS

Cells, viruses, and transfections. 293-EBV2089, 293-D3, and 293T cells were cultured at 37°C in a 5% CO2-humidified atmosphere in high glucose DMEM supplemented with 10% fetal bovine serum (FBS) and 1% penicillin, streptomycin, and L-glutamine (P/S/G). MutuI cells were maintained in RPMI 1640 supplemented with 10% FBS and 1% P/S/G. For preparation of lentiviruses, 293T cells were plated in 15-cm plates in complete media and transfected using polyethylenimine (PEI) with 15 μg lentivector (pLCE), 9 μg pDeltaR8.75, and 6 μg pMD2G. Media was changed between 8 h and 16 h posttransfection. Lentiviral particles were harvested by sterile filtration of the supernatant using a 0.45-micron filter at 48- and 96-h posttransfection and used to transduce 293-D3 cells.

Viral loads. To screen EBV miRNAs for reactivation phenotypes, 293-2,089 cells were plated in 12-well plates and transfected with 1 μg pLCE-based miRNA vector and 200 ng pSG5-Zta using Lipofectamine 2000 (ThermoFisher). To assay EBV loads, genomic DNA was isolated from cells at 48–72 h using DNAzol (Thermofisher). 100 ng of genomic DNA were analyzed by qPCR using primers to the LMP1 region and normalized to GAPDH levels as previously described (24). For viral loads in supernatant, cells were transfected with empty pcDNA3 or pcDNA3-BZLF1-FL. 24 h later, cells were washed by PBS and fresh DMEM complete media were added. Two days later supernatant was collected, and cells and debris were removed by high-speed centrifugation. Virion DNA was extracted using the Wizard DNA Purification kit following standard protocols (Promega). Viral loads were determined by qPCR for LMP1 copies using LMP1 standard curve. All PCRs were performed in technical replicates.

Plasmids. pLCE-based EBV miRNA expression vectors are previously described (24, 31, 33, 55). To generate constructs for miR-BHRF1-3 variants, gene fragments were synthesized and cloned into pLCE at XhoI/XbaI sites within the 3′UTR of eGFP. pSG5-Zta is previously described in (61). pcDNA3-BZLF1-FL (contains the full length BZLF1 gene with the 3′UTR) and pcDNA3-BZLF1dUTR were PCR amplified from MutuI genomic DNA and cloned into pcDNA3 at XhoI/XbaI sites. psicheck2-based BZLF1 3′UTR reporters were generated using PCR amplicons from MutuI or rLCV genomic DNA (WT) or synthesized gene fragments (mt and SNP) and cloned into psicheck2 at XhoI/NotI sites. Lentiviral vector miRNA sponge inhibitor (pLCE-BHRF1-3spg) contains nine imperfect, tandem target sites for miR-BHRF1-3 cloned into the GFP 3′UTR as previously described (24). The control sponge (pLCE-CXCR4) lacks miRNA binding sites and is previously described (24).

Quantitative RT-PCR (reverse transcription-PCR). For gene expression analysis, total RNA was extracted using TRIzol (Thermofisher), DNase-treated, and reversed transcribed using MultiScribe (Thermofisher) with random hexamers. Cellular and viral genes were detected using PowerUp SYBR green qPCR (Thermofisher). For miRNA expression analysis, total RNA was reverse transcribed using miRNA-specific TaqMan (Thermofisher) primers and miRNAs were detected using miRNA-specific TaqMan probes and TaqMan Universal PCR mastermix (Thermofisher). Oligonucleotides sequences are available upon request. All PCRs were performed in technical replicates (duplicates or triplicates).

Luciferase reporter assays. 293T cells were co-transfected with 20 ng of 3′UTR reporter and 250 ng of control or miRNA expression vector using Lipofectamine2000 (Thermofisher). 48–72 h posttransfection, cells were lysed in 1X passive lysis buffer (Promega), and lysates assayed for dual luciferase activity using the Dual Luciferase Reporter Assay System (Promega). All values are reported as relative light units (RLU) normalized to renilla luciferase internal control and shown relative to control empty vector.

Western blot analysis. Cell lysates were prepared using RIPA lysis buffer and protein concentrations were determined using a BCA protein quantification kit (Pierce). 10 μg of total protein lysate were resolved on 4–20% Tris-glycine SDS-PAGE and transferred onto Immobilon PVDF membranes. Blots were probed with primary antibodies to EBV ZEBRA (BZLF1) (sc-53904, Santa Cruz), or Beta-actin (sc-47778, Santa Cruz), followed by horseradish peroxidase conjugated secondary antibody anti-mouse IgG. Blots were developed with enhanced chemiluminescent substrate (Pierce). Band intensities were quantified using NIH ImageJ, normalized to loading controls, and reported relative to control cells.

Sequence analysis of the miR-BHRF1-3 and BZLF1 loci. Sequences for 880 EBV genomes (at least 169,000 nucleotides in length) were obtained through the NCBI nucleotide database. Regions encompassing the miR-BHRF1-3 precursor and the BZLF1 3′UTR were extracted and alignments were performed using Clustal Omega (version 1.2.4) multiple sequence alignment. The full list of viral genome accession numbers used for sequence alignments is available upon request.

PAR-CLIP and bioinformatics analysis. PAR-CLIP analysis for MutuI cells was performed as previously described (31, 33). Briefly, latent cells were spun down, resuspended at 2 $\times$ 10^6 cells/ml in complete media, and pretreated for 2 h with 100 uM 4SU prior to the addition of 2.5 μg/ml soluble anti-IgM (Sigma) for 20 h. After cross-linking at UV 365 nm, Ago-bound RNAs were immunopurified with pan-Ago antibody 2A8 (diagenode) and ligated to sequencing adapters. Sequencing was performed on the Illumina Hiseq2000 by the OHSU MPSSR. Raw fastq files were concatenated, adapters were clipped, and 67,167,673 sequences were collapsed using the FASTX-toolkit (http://hannonlab.cshl.edu/fastx_toolkit/), discarding

sequences that contained an N or were <12 nt after adapters were removed. 37,595,881 reads passed initial quality control and were mapped to either HG19 or the EBV (KC207814.1) genome. Mapped reads were analyzed by PARalyzer (40), requiring a minimum read count of three reads per cluster. 9,667,065 reads mapped to the EBV genome. In total, 28,835 cellular Ago interaction sites and 5,544 EBV Ago interaction sites (minimal length cutoff of 12 nucleotides) were identified by PARalyzer. Seed match sites for EBV miR-BHRF1-3 were subsequently annotated. PAR-CLIP sequencing data can be accessed through NCBI short read archive (SRA; BioProject PRJNA773484).

Statistical analyses. Luciferase and PCR data are reported as mean of at least three independent experiments (unless otherwise stated) with standard deviations. Statistical significance was determined by paired Student's *t* test, performed in GraphPad Prism 9.0.1 (GraphPad Software, USA), and values $P < 0.05$ were considered significant.

Data availability. PAR-CLIP sequencing data with BioProject were submitted under accession number PRJNA773484.

ACKNOWLEDGMENTS

This work was supported by startup funds from the Vaccine and Gene Therapy Institute and R01 AI143620 from the National Institute of Allergy and Infectious Diseases to R.L.S. We thank members of the Skalsky lab, specifically Rodney Kincaid, for critical readings of the manuscript, Kelley Bastin for assistance with qPCR, and Divya Jeyasingh, a previous summer undergraduate student, for assistance with EBV sequence annotations.

REFERENCES

1. Young LS, Rickinson AB. 2004. Epstein-Barr virus: 40 years on. Nat Rev Cancer 4:757–768. https://doi.org/10.1038/nrc1452.
2. Rickinson AB, Kieff E. 2007. Epstein-Barr virus, p 2655–2700. *In* Knipe DM, Howley PM, Griffin DE, Lamb RA, Martin MA, Roizman B, Straus SE (ed), Fields virology, 5th ed, vol 2. Lippincott Williams & Wilkins, Philadelphia.
3. Laichalk LL, Thorley-Lawson DA. 2005. Terminal differentiation into plasma cells initiates the replicative cycle of Epstein-Barr virus in vivo. J Virol 79:1296–1307. https://doi.org/10.1128/JVI.79.2.1296-1307.2005.
4. Bhende PM, Seaman WT, Delecluse HJ, Kenney SC. 2004. The EBV lytic switch protein, Z, preferentially binds to and activates the methylated viral genome. Nat Genet 36:1099–1104. https://doi.org/10.1038/ng1424.
5. Bergbauer M, Kalla M, Schmeinck A, Gobel C, Rothbauer U, Eck S, Benet-Pages A, Strom TM, Hammerschmidt W. 2010. CpG-methylation regulates a class of Epstein-Barr virus promoters. PLoS Pathog 6:e1001114. https://doi.org/10.1371/journal.ppat.1001114.
6. McKenzie J, El-Guindy A. 2015. Epstein-Barr Virus Lytic Cycle Reactivation. Curr Top Microbiol Immunol 391:237–261. https://doi.org/10.1007/978-3-319-22834-1_8.
7. Kenney SC, Mertz JE. 2014. Regulation of the latent-lytic switch in Epstein-Barr virus. Semin Cancer Biol 26:60–68. https://doi.org/10.1016/j.semcancer.2014.01.002.
8. Flemington E, Speck SH. 1990. Autoregulation of Epstein-Barr virus putative lytic switch gene BZLF1. J Virol 64:1227–1232. https://doi.org/10.1128/JVI.64.3.1227-1232.1990.
9. Munz C. 2021. The Role of Lytic Infection for Lymphomagenesis of Human gamma-Herpesviruses. Front Cell Infect Microbiol 11:605258. https://doi.org/10.3389/fcimb.2021.605258.
10. Hong GK, Gulley ML, Feng WH, Delecluse HJ, Holley-Guthrie E, Kenney SC. 2005. Epstein-Barr virus lytic infection contributes to lymphoproliferative disease in a SCID mouse model. J Virol 79:13993–14003. https://doi.org/10.1128/JVI.79.22.13993-14003.2005.
11. Ma SD, Hegde S, Young KH, Sullivan R, Rajesh D, Zhou Y, Jankowska-Gan E, Burlingham WJ, Sun X, Gulley ML, Tang W, Gumperz JE, Kenney SC. 2011. A new model of Epstein-Barr virus infection reveals an important role for early lytic viral protein expression in the development of lymphomas. J Virol 85:165–177. https://doi.org/10.1128/JVI.01512-10.
12. Ma SD, Yu X, Mertz JE, Gumperz JE, Reinheim E, Zhou Y, Tang W, Burlingham WJ, Gulley ML, Kenney SC. 2012. An Epstein-Barr Virus (EBV) mutant with enhanced BZLF1 expression causes lymphomas with abortive lytic EBV infection in a humanized mouse model. J Virol 86:7976–7987. https://doi.org/10.1128/JVI.00770-12.
13. Romero-Masters JC, Ohashi M, Djavadian R, Eichelberg MR, Hayes M, Zumwalde NA, Bristol JA, Nelson SE, Ma S, Ranheim EA, Gumperz JE, Johannsen EC, Kenney SC. 2020. An EBNA3A-mutated Epstein-Barr virus retains the capacity for lymphomagenesis in a cord blood-humanized mouse model. J Virol 94. https://doi.org/10.1128/JVI.02168-19.
14. Okuno Y, Murata T, Sato Y, Muramatsu H, Ito Y, Watanabe T, Okuno T, Murakami N, Yoshida K, Sawada A, Inoue M, Kawa K, Seto M, Ohshima K, Shiraishi Y, Chiba K, Tanaka H, Miyano S, Narita Y, Yoshida M, Goshima F, Kawada JI, Nishida T, Kiyoi H, Kato S, Nakamura S, Morishima S, Yoshikawa T, Fujiwara S, Shimizu N, Isobe Y, Noguchi M, Kikuta A, Iwatsuki K, Takahashi Y, Kojima S, Ogawa S, Kimura H. 2019. Defective Epstein-Barr virus in chronic active infection and haematological malignancy. Nat Microbiol 4:404–413. https://doi.org/10.1038/s41564-018-0334-0.
15. Munz C. 2019. Latency and lytic replication in Epstein-Barr virus-associated oncogenesis. Nat Rev Microbiol 17:691–700. https://doi.org/10.1038/s41579-019-0249-7.
16. Coghill AE, Hildesheim A. 2014. Epstein-Barr virus antibodies and the risk of associated malignancies: review of the literature. Am J Epidemiol 180:687–695. https://doi.org/10.1093/aje/kwu176.
17. Cao SM, Liu Z, Jia WH, Huang QH, Liu Q, Guo X, Huang TB, Ye W, Hong MH. 2011. Fluctuations of epstein-barr virus serological antibodies and risk for nasopharyngeal carcinoma: a prospective screening study with a 20-year follow-up. PLoS One 6:e19100. https://doi.org/10.1371/journal.pone.0019100.
18. Bristol JA, Djavadian R, Albright ER, Coleman CB, Ohashi M, Hayes M, Romero-Masters JC, Barlow EA, Farrell PJ, Rochford R, Kalejta RF, Johannsen EC, Kenney SC. 2018. A cancer-associated Epstein-Barr virus BZLF1 promoter variant enhances lytic infection. PLoS Pathog 14:e1007179. https://doi.org/10.1371/journal.ppat.1007179.
19. Bartel DP. 2009. MicroRNAs: target recognition and regulatory functions. Cell 136:215–233. https://doi.org/10.1016/j.cell.2009.01.002.
20. Agarwal V, Bell GW, Nam JW, Bartel DP. 2015. Predicting effective microRNA target sites in mammalian mRNAs. Elife 4:e05005. https://doi.org/10.7554/eLife.05005.
21. Bouvet M, Voigt S, Tagawa T, Albanese M, Chen YA, Chen Y, Fachko DN, Pich D, Gobel C, Skalsky RL, Hammerschmidt W. 2021. Multiple viral microRNAs regulate interferon release and signaling early during infection with Epstein-Barr virus. mBio 12:e03440-20. https://doi.org/10.1128/mBio.03440-20.
22. Iizasa H, Kim H, Kartika AV, Kanehiro Y, Yoshiyama H. 2020. Role of viral and host microRNAs in immune regulation of Epstein-Barr virus-associated diseases. Front Immunol 11:367. https://doi.org/10.3389/fimmu.2020.00367.
23. Murer A, Ruhl J, Zbinden A, Capaul R, Hammerschmidt W, Chijioke O, Munz C. 2019. MicroRNAs of Epstein-Barr virus attenuate T-cell-mediated immune control in vivo. mBio 10:e01941-18. https://doi.org/10.1128/mBio.01941-18.
24. Chen Y, Fachko D, Ivanov NS, Skinner CM, Skalsky RL. 2019. Epstein-Barr virus microRNAs regulate B cell receptor signal transduction and lytic reactivation. PLoS Pathog 15:e1007535. https://doi.org/10.1371/journal.ppat.1007535.
25. Amoroso R, Fitzsimmons L, Thomas WA, Kelly GL, Rowe M, Bell AI. 2011. Quantitative studies of Epstein-Barr virus-encoded microRNAs provide

novel insights into their regulation. J Virol 85:996–1010. https://doi.org/10.1128/JVI.01528-10.
26. Barth S, Pfuhl T, Mamiani A, Ehses C, Roemer K, Kremmer E, Jaker C, Hock J, Meister G, Grasser FA. 2008. Epstein-Barr virus-encoded microRNA miR-BART2 down-regulates the viral DNA polymerase BALF5. Nucleic Acids Res 36:666–675. https://doi.org/10.1093/nar/gkm1080.
27. Jung YJ, Choi H, Kim H, Lee SK. 2014. MicroRNA miR-BART20-5p stabilizes Epstein-Barr virus latency by directly targeting BZLF1 and BRLF1. J Virol 88:9027–9037. https://doi.org/10.1128/JVI.00721-14.
28. Iizasa H, Wulff BE, Alla NR, Maragkakis M, Megraw M, Hatzigeorgiou A, Iwakiri D, Takada K, Wiedmer A, Showe L, Lieberman P, Nishikura K. 2010. Editing of EBV-encoded BART6 microRNAs controls their dicer targeting and consequently affects viral latency. J Biol Chem 285:33358–33370. https://doi.org/10.1074/jbc.M110.138362.
29. Qiu J, Thorley-Lawson DA. 2014. EBV microRNA BART 18-5p targets MAP3K2 to facilitate persistence in vivo by inhibiting viral replication in B cells. Proc Natl Acad Sci U S A 111:11157–11162. https://doi.org/10.1073/pnas.1406136111.
30. Feederle R, Linnstaedt SD, Bannert H, Lips H, Bencun M, Cullen BR, Delecluse HJ. 2011. A viral microRNA cluster strongly potentiates the transforming properties of a human herpesvirus. PLoS Pathog 7:e1001294. https://doi.org/10.1371/journal.ppat.1001294.
31. Skalsky RL, Kang D, Linnstaedt SD, Cullen BR. 2014. Evolutionary conservation of primate lymphocryptovirus microRNA targets. J Virol 88:1617–1635. https://doi.org/10.1128/JVI.02071-13.
32. Feederle R, Haar J, Bernhardt K, Linnstaedt SD, Bannert H, Lips H, Cullen BR, Delecluse HJ. 2011. The members of an Epstein-Barr virus microRNA cluster cooperate to transform B lymphocytes. J Virol 85:9801–9810. https://doi.org/10.1128/JVI.05100-11.
33. Skalsky RL, Corcoran DL, Gottwein E, Frank CL, Kang D, Hafner M, Nusbaum JD, Feederle R, Delecluse HJ, Luftig MA, Tuschl T, Ohler U, Cullen BR. 2012. The viral and cellular microRNA targetome in lymphoblastoid cell lines. PLoS Pathog 8:e1002484. https://doi.org/10.1371/journal.ppat.1002484.
34. Albanese M, Tagawa T, Bouvet M, Maliqi L, Lutter D, Hoser J, Hastreiter M, Hayes M, Sugden B, Martin L, Moosmann A, Hammerschmidt W. 2016. Epstein-Barr virus microRNAs reduce immune surveillance by virus-specific CD8+ T cells. Proc Natl Acad Sci U S A 113:E6467–E6475. https://doi.org/10.1073/pnas.1605884113.
35. Bernhardt K, Haar J, Tsai MH, Poirey R, Feederle R, Delecluse HJ. 2016. A viral microRNA cluster regulates the expression of PTEN, p27 and of a bcl-2 Homolog. PLoS Pathog 12:e1005405. https://doi.org/10.1371/journal.ppat.1005405.
36. Bellare P, Ganem D. 2009. Regulation of KSHV lytic switch protein expression by a virus-encoded microRNA: an evolutionary adaptation that fine-tunes lytic reactivation. Cell Host Microbe 6:570–575. https://doi.org/10.1016/j.chom.2009.11.008.
37. Grey F, Meyers H, White EA, Spector DH, Nelson J. 2007. A human cytomegalovirus-encoded microRNA regulates expression of multiple viral genes involved in replication. PLoS Pathog 3:e163. https://doi.org/10.1371/journal.ppat.0030163.
38. Murphy E, Vanicek J, Robins H, Shenk T, Levine AJ. 2008. Suppression of immediate-early viral gene expression by herpesvirus-coded microRNAs: implications for latency. Proc Natl Acad Sci U S A 105:5453–5458. https://doi.org/10.1073/pnas.0711910105.
39. Umbach JL, Kramer MF, Jurak I, Karnowski HW, Coen DM, Cullen BR. 2008. MicroRNAs expressed by herpes simplex virus 1 during latent infection regulate viral mRNAs. Nature 454:780–783. https://doi.org/10.1038/nature07103.
40. Corcoran DL, Georgiev S, Mukherjee N, Gottwein E, Skalsky RL, Keene JD, Ohler U. 2011. PARalyzer: definition of RNA binding sites from PAR-CLIP short-read sequence data. Genome Biol 12:R79. https://doi.org/10.1186/gb-2011-12-8-r79.
41. Majoros WH, Ohler U. 2007. Spatial preferences of microRNA targets in 3' untranslated regions. BMC Genomics 8:152. https://doi.org/10.1186/1471-2164-8-152.
42. Han SJ, Marshall V, Barsov E, Quinones O, Ray A, Labo N, Trivett M, Ott D, Renne R, Whitby D. 2013. Kaposi's sarcoma-associated herpesvirus microRNA single-nucleotide polymorphisms identified in clinical samples can affect microRNA processing, level of expression, and silencing activity. J Virol 87:12237–12248. https://doi.org/10.1128/JVI.01202-13.
43. Marshall VA, Labo N, Sztuba-Solinska J, Cornejo Castro EM, Aleman K, Wyvill KM, McNamara L, Le Grice SFJ, Yarchoan R, Uldrick TS, MacPhail P, Polizzotto MN, Whitby D. 2018. Polymorphisms in KSHV-encoded microRNA sequences affect levels of mature viral microRNA in Kaposi Sarcoma lesions. Oncotarget 9:35856–35869. https://doi.org/10.18632/oncotarget.26321.
44. Correia S, Palser A, Elgueta Karstegl C, Middeldorp JM, Ramayanti O, Cohen JI, Hildesheim A, Fellner MD, Wiels J, White RE, Kellam P, Farrell PJ. 2017. Natural variation of Epstein-Barr virus genes, proteins, and primary microRNA. J Virol 91. https://doi.org/10.1128/JVI.00375-17.
45. Chen SJ, Chen GH, Chen YH, Liu CY, Chang KP, Chang YS, Chen HC. 2010. Characterization of Epstein-Barr virus miRNAome in nasopharyngeal carcinoma by deep sequencing. PLoS One 5:e12745. https://doi.org/10.1371/journal.pone.0012745.
46. Pratt ZL, Kuzembayeva M, Sengupta S, Sugden B. 2009. The microRNAs of Epstein-Barr virus are expressed at dramatically differing levels among cell lines. Virology 386:387–397. https://doi.org/10.1016/j.virol.2009.01.006.
47. Sievers F, Wilm A, Dineen D, Gibson TJ, Karplus K, Li W, Lopez R, McWilliam H, Remmert M, Soding J, Thompson JD, Higgins DG. 2011. Fast, scalable generation of high-quality protein multiple sequence alignments using Clustal Omega. Mol Syst Biol 7:539. https://doi.org/10.1038/msb.2011.75.
48. Correia S, Bridges R, Wegner F, Venturini C, Palser A, Middeldorp JM, Cohen JI, Lorenzetti MA, Bassano I, White RE, Kellam P, Breuer J, Farrell PJ. 2018. Sequence variation of Epstein-Barr virus: Viral types, geography, codon usage, and diseases. J Virol 92:e01132-18. https://doi.org/10.1128/JVI.01132-18.
49. Zuker M. 2003. Mfold web server for nucleic acid folding and hybridization prediction. Nucleic Acids Res 31:3406–3415. https://doi.org/10.1093/nar/gkg595.
50. Kamperschroer C, Gosink MM, Kumpf SW, O'Donnell LM, Tartaro KR. 2016. The genomic sequence of lymphocryptovirus from cynomolgus macaque. Virology 488:28–36. https://doi.org/10.1016/j.virol.2015.10.025.
51. Bai Z, Huang Y, Li W, Zhu Y, Jung JU, Lu C, Gao SJ. 2014. Genomewide mapping and screening of Kaposi's sarcoma-associated herpesvirus (KSHV) 3' untranslated regions identify bicistronic and polycistronic viral transcripts as frequent targets of KSHV microRNAs. J Virol 88:377–392. https://doi.org/10.1128/JVI.02689-13.
52. Lin X, Liang D, He Z, Deng Q, Robertson ES, Lan K. 2011. miR-K12-7-5p encoded by Kaposi's sarcoma-associated herpesvirus stabilizes the latent state by targeting viral ORF50/RTA. PLoS One 6:e16224. https://doi.org/10.1371/journal.pone.0016224.
53. Seto E, Moosmann A, Gromminger S, Walz N, Grundhoff A, Hammerschmidt W. 2010. Micro RNAs of Epstein-Barr virus promote cell cycle progression and prevent apoptosis of primary human B cells. PLoS Pathog 6:e1001063. https://doi.org/10.1371/journal.ppat.1001063.
54. Lin X, Tsai MH, Shumilov A, Poirey R, Bannert H, Middeldorp JM, Feederle R, Delecluse HJ. 2015. The Epstein-Barr virus BART miRNA cluster of the M81 strain modulates multiple functions in primary B cells. PLoS Pathog 11:e1005344. https://doi.org/10.1371/journal.ppat.1005344.
55. Kang D, Skalsky RL, Cullen BR. 2015. EBV BART MicroRNAs target multiple pro-apoptotic cellular genes to promote epithelial cell survival. PLoS Pathog 11:e1004979. https://doi.org/10.1371/journal.ppat.1004979.
56. Riley KJ, Rabinowitz GS, Yario TA, Luna JM, Darnell RB, Steitz JA. 2012. EBV and human microRNAs co-target oncogenic and apoptotic viral and human genes during latency. EMBO J 31:2207–2221. https://doi.org/10.1038/emboj.2012.63.
57. Munz C. 2021. Immune escape by non-coding RNAs of the Epstein Barr virus. Front Microbiol 12:657387. https://doi.org/10.3389/fmicb.2021.657387.
58. Kimura H, Cohen JI. 2017. Chronic Active Epstein-Barr Virus Disease. Front Immunol 8:1867. https://doi.org/10.3389/fimmu.2017.01867.
59. Xia T, O'Hara A, Araujo I, Barreto J, Carvalho E, Sapucaia JB, Ramos JC, Luz E, Pedroso C, Manrique M, Toomey NL, Brites C, Dittmer DP, Harrington WJ. Jr, 2008. EBV microRNAs in primary lymphomas and targeting of CXCL-11 by ebv-mir-BHRF1-3. Cancer Res 68:1436–1442. https://doi.org/10.1158/0008-5472.CAN-07-5126.
60. Lee YE, He HL, Chen TJ, Lee SW, Chang IW, Hsing CH, Li CF. 2015. The prognostic impact of RAP2A expression in patients with early and locoregionally advanced nasopharyngeal carcinoma in an endemic area. Am J Transl Res 7:912–921.
61. Sarisky RT, Gao Z, Lieberman PM, Fixman ED, Hayward GS, Hayward SD. 1996. A replication function associated with the activation domain of the Epstein-Barr virus Zta transactivator. J Virol 70:8340–8347. https://doi.org/10.1128/JVI.70.12.8340-8347.1996.